Control of Radioactivity Pharmacokinetics of 99m Tc–HYNIC-Labeled Polypeptides Derivatized with Ternary Ligand Complexes

ARTICLE *in* BIOCONJUGATE CHEMISTRY · MAY 2002

Impact Factor: 4.51 · DOI: 10.1021/bc010043k · Source: PubMed

9 AUTHORS, INCLUDING:

Yasushi Arano
Chiba University
217 PUBLICATIONS **2,059** CITATIONS

SEE PROFILE

Takahiro Mukai
Nagoya Institute of Technology
230 PUBLICATIONS **3,178** CITATIONS

SEE PROFILE

Kazuma Ogawa
Kanazawa University
67 PUBLICATIONS **911** CITATIONS

SEE PROFILE

Control of Radioactivity Pharmacokinetics of ^{99m}Tc−HYNIC-Labeled Polypeptides Derivatized with Ternary Ligand Complexes

Masahiro Ono,[†] Yasushi Arano,[‡] Takahiro Mukai,[§] Tsuneo Saga,[§] Yasushi Fujioka,[†] Kazuma Ogawa,[†] Hidekazu Kawashima,[†] Junji Konishi,[§] and Hideo Saji*,[†]

Department of Patho-Functional Bioanalysis, Graduate School of Pharmaceutical Sciences, Kyoto University, Yoshida Shimoadachi-cho, Sakyo-ku, Kyoto 606-8501, Department of Molecular Imaging and Radiotherapy, Graduate School of Pharmaceutical Sciences, Chiba University, 1-33 Yayoi-cho, Inage-ku, Chiba 263-8522, and Department of Nuclear Medicine and Diagnostic Imaging, Graduate School of Medicine, Kyoto University, Shogoin Kawahara-cho, Sakyo-ku, Kyoto 606-8507, Japan. Received March 28, 2001; Revised Manuscript Received October 23, 2001

An enhancement of the target/nontarget ratio of radioactivity levels enables reliable diagnosis and therapy using polypeptide radiopharmaceuticals in nuclear medicine. In the present study, we investigated the effects of the physicochemical properties of radiometabolites on the radioactivity pharmacokinetics after administration of ^{99m}Tc-labeled polypeptides using 6-hydrazinopyridine-3-carboxylic acid (HYNIC). Four ternary ligands (L) [3-benzoylpyridine (BP), 3-acetylpyridine (AP), 3-nicotinic acid (NIC), pyridine (PY)] with different lipophilicity were selected as coligands for the preparation of ^{99m}Tc−HYNIC-polypeptides. Each of the ternary ligands tested provided ^{99m}Tc−HYNIC-labeled galactosyl-neoalbumin (NGA) and Fab fragments of high stability with high radiochemical purity. Moreover, after administration of each ^{99m}Tc−HYNIC-labeled NGA into normal mice, the respective ternary ligand [^{99m}Tc](HYNIC−lysine)(tricine)(L) complexes were generated as final radiometabolites in the hepatic lysosome. The partition coefficients of [^{99m}Tc](HYNIC−lysine)(tricine)-(BP), [^{99m}Tc](HYNIC−lysine)(tricine)(AP), [^{99m}Tc](HYNIC−lysine)(tricine)(NIC), and [^{99m}Tc](HYNIC−lysine)(tricine)(PY) were determined to be −2.21, −2.37, −2.93, and −2.73, respectively. Elimination rates of these radiometabolites from the lysosome were enhanced in the order of increasing lipophilicity of the radiometabolites. After injection of the four ^{99m}Tc−HYNIC-labeled Fab fragments into normal mice, blood clearances of radioactivity were similar while radioactivity elimination rates from the kidney were enhanced in the order of increasing lipophilicity of the radiometabolites. The present study indicated that the lipophilicity of the radiometabolites constitutes one important factor affecting their elimination rates from the tissues. Thus, as ternary ligands facilitate alteration of the physicochemical properties of radiometabolites, the use of ternary ligand complexes might be applicable for controlling the pharmacokinetics of ^{99m}Tc-labeled polypeptides.

INTRODUCTION

Radiopharmaceuticals derived from polypeptides and peptides have been shown to be useful for both diagnostic and therapeutic applications. However, high-level and prolonged retention of radioactivity has been observed in nontarget tissues such as the liver and kidney when these radiopharmaceuticals are administered. This results in a high background radioactivity in imaging diagnosis and also increases the radiation dose to the patients, thus limiting their therapeutic uses.

To decrease the radioactivity levels in nontarget tissues, attempts to conjugate polypeptides with a radiolabel via a metabolizable linkage have been made (*1*−*5*). However, the following criteria should be addressed for application of radiolabeling reagents with a metabolizable linkage to polypeptides. One important point is whether the radiolabeled compound released from the polypeptides by cleavage of the labile bond can rapidly penetrate the lysosomal membrane. Another point to be considered is whether the metabolizable linkage is stable enough in plasma so as not to impair the radioactivity in the target delivered by the polypeptides. Although radiolabeling reagents with a metabolizable linkage satisfy these criteria, they cannot be applied to polypeptides that are internalized within target cells.

Another solution to the high radioactivity levels in nontarget tissues appears to be the chemical modification of polypeptides and peptides. This strategy involves modification of isoelectric points of (poly)peptides by acylating amine residues, attachment of negatively charged polymer, or substitution of N-terminal amino acid with an acidic amino acid (*6*−*9*). Although these methods can be applied to polypeptides that are internalized within target cells, long-term retention of the radioactivity in the target tissues is required for further enhancement of the target/nontarget ratio.

Recent studies on the metabolism of radiolabeled polypeptides have shown that in vivo behaviors of radiometabolites generated after lysosomal proteolysis play a critical role in determining the radioactivity levels in tissues (*10*−*13*). These findings provide the following approaches to enhance the target/nontarget ratio of

* To whom correspondence should be addressed. Telephone: 81−75−753−4567; fax: 81−75−753−4568; e-mail: hsaji@pharm.kyoto-u.ac.jp.

[†] Department of Patho-Functional Bioanalysis, Graduate School of Pharmaceutical Sciences, Kyoto University.

[‡] Chiba University.

[§] Department of Nuclear Medicine and Diagnostic Imaging, Graduate School of Medicine, Kyoto University.

10.1021/bc010043k CCC: $22.00
Published on Web 04/09/2002

radioactivity level. When applied to polypeptides such as antibodies against solid tumors, which are not or are only slowly internalized within target cells, generation of radiometabolites that are eliminated rapidly from the tissues constitutes one useful approach. Radiolabeled polypeptides remain bound to the surface of target cells, while their radiometabolites generated after lysosomal proteolysis are eliminated rapidly from nontarget tissues. As a consequence, the target/nontarget ratio is increased. On the other hand, when applied to internalizable (poly)-peptides within target cells, generation of radiometabolites that are eliminated slowly from the tissues would be required to prolong radioactivity retention in target tissues. Therefore, it is important for enhancement of the target/nontarget ratio to control the in vivo behaviors of radiometabolites generated after lysosomal proteolysis of polypeptide radiopharmaceuticals regardless of whether the parental molecules are internalized into target cells. However, the relationships between the physicochemical properties of radiometabolites and their elimination rates from the tissues remain unclear.

6-Hydrazinopyridine-3-carboxylic acid (HYNIC) is a representative agent used to prepare technetium-99m (^{99m}Tc)-labeled (poly)peptides with tricine as a coligand (*14*−*18*). However, it was found that the complex [^{99m}Tc]-(HYNIC)(tricine)$_2$, which is not stable and exists as multiple species, could affect the pharmacokinetics of ^{99m}Tc-labeled (poly)peptides and their radiometabolites due to exchange reaction of tricine with protein in the plasma and tissues (*19*−*22*). To decrease the problems associated with ^{99m}Tc−HYNIC-labeled small peptides, Liu et al. exploited several pyridine derivatives as ternary ligands to form ternary ligand complexes, [^{99m}Tc](HYNIC-peptide)(tricine)(pyridine derivative), with high stability and fewer isomers (*23*). On the basis of these findings, we applied a preformed chelate of tetrafluorophenol active ester of the ternary ligand complex [^{99m}Tc](HYNIC)-(tricine)[3-benzoylpyridine (BP)] to prepare ^{99m}Tc-labeled polypeptides (24). Our previous study using galactosyl-neoglycoalbumin (NGA) indicated that [^{99m}Tc](HYNIC−lysine)(tricine)(BP) was generated as a major radiometabolite in the liver and that the binding of this metabolite with lysosomal proteins was low. In addition, little plasma protein binding was observed in ^{99m}Tc−HYNIC-labeled Fab fragment derivatized with this ternary ligand complex. These findings indicated that the pyridine derivatives could serve as highly stable coligands for preparing ^{99m}Tc−HYNIC-labeled polypeptides and that the use of various pyridine derivatives would generate radiometabolites with different physicochemical properties in the tissues.

In the present study, four pyridine derivatives [BP, 3-acetylpyridine (AP), 3-nicotinic acid (NIC) and pyridine (PY)] with different lipophilicity were selected as ternary ligands to prepare ^{99m}Tc−HYNIC-labeled polypeptides. We investigated the effects of lipophilicity of the radiometabolites on the radioactivity pharmacokinetics after injection of ^{99m}Tc−HYNIC-labeled NGA. In addition, the radioactivity elimination from the kidney after injection of four ^{99m}Tc−HYNIC-labeled Fab fragments was also estimated along with the blood clearance.

MATERIALS AND METHODS

Reagents and Chemicals. [^{99m}Tc]Pertechnetate ($^{99m}TcO_4^-$) was eluted in saline solution on a daily basis from Daiichi Radioisotope Laboratory generators (Chiba, Japan). Na[^{125}I] was obtained from the Daiichi Kagaku (Tokyo, Japan) and was diluted with 0.1 M phosphate buffer (pH 7.4) to 3.7 MBq/μL. Reversed phase high performance liquid chromatography (RP-HPLC) was performed with a Cosmosil 5 C_{18}-AR-300 column (4.6 × 150 mm, Nacalai Tesque, Kyoto, Japan) at a flow rate of 1.0 mL/min with a gradient mobile phase starting from 90% A (0.1% aqueous trifluoroacetic acid) and 10% B (acetonitrile with 0.1% trifluoroacetic acid) to 50% A and 50% B at 20 min and to 100% B at 30 min (solvent system 1). RP-HPLC was also performed with a gradient mobile phase starting from 100% A to 100% B in 30 min (solvent system 2). Size-exclusion HPLC (SE-HPLC) was performed using a 5 Diol-300 column (7.5 × 600 mm, Nacalai Tesque) connected to a 5 Diol-300 guard column (7.5 × 50 mm, Nacalai Tesque), eluted with 0.1 M phosphate buffer (pH 6.8) at a flow rate of 1 mL/min. The eluent was collected with a fraction collector (RediFrac; Pharmacia Biotech, Tokyo, Japan) at 30-s intervals, and the radioactivity levels in each fraction (500 μL) were determined with an auto well counter (ARC-2000; Aloka, Tokyo). The radioactivity of liver homogenates was analyzed by gel permeation chromatography (GPC) using a Sephadex G-50 (Pharmacia Biotech) column (18 × 400 mm) equilibrated and eluted with 0.1 M phosphate buffer (pH 6.8) at a flow rate of 1 mL/min. The eluent was collected with a fraction collector at 2.5-min intervals, and the radioactivity levels in each fraction (2.5 mL) were measured with an auto well counter. TLC analyses were performed with silica plates (Merck Art 5553) with a mixture of 10% aqueous ammonium chloride−methanol (1:1) or saline as the developing solvent. Cellulose acetate electrophoresis (CAE) strips were run in veronal buffer (pH 8.6, $I = 0.05$) at a constant current of 0.8 mA for 30 min. Proton nuclear magnetic resonance (^{1}H NMR) spectra were recorded on a Bruker AC-200 spectrometer, and the chemical shifts are reported in ppm downfield from an internal tetramethylsilane standard. Fast atom bombardment mass spectra (FAB-MS) were obtained with a JMS−HX/HX 110 A model (JEOL Ltd., Tokyo, Japan). Tricine, BP, AP, NIC, and PY were purchased from Nacalai Tesque, and other reagents were of reagent grade and used as received. To facilitate collection of urine and feces after administration of radiolabeled polypeptides, mice were housed in metabolic cages (Metabolica, MM type; Sugiyama-Gen Iriki Co. Ltd., Tokyo, Japan).

Synthesis of Galactosyl-neoglycoalbumin (NGA). Cyanomethyl-2,3,4,6-tetra-*O*-acetyl-1-β-galactopyranoside, synthesized according to the procedure of Lee et al. (*25*), was conjugated with human serum albumin (HSA, A-3782; Sigma Co. St. Louis, MO), according to the procedure of Stowell et al. (*26*). The phenol−sulfuric acid reaction (*27*) indicated that 43 galactose units were attached to each HSA molecule.

Tumor and Monoclonal Antibodies. KT005-cloned human osteogenic sarcoma was maintained by serial sc transplantation in athymic mice. Pieces of tumor tissue (∼0.5 g) at ∼2.5 weeks postimplantation were used for the in vivo study**.** The monoclonal antibody against osteogenic sarcoma (OST7, IgG_1), generated by the standard hybridoma technique, was purified by ammonium sulfate precipitation with subsequent protein A affinity chromatography (Pharmacia Biotech), as reported previously (*28*). The Fab fragment was prepared by the standard procedure using papain (*29*).

Synthesis of ^{99m}Tc−HYNIC Ternary Ligand Complexes. 2,3,5,6-Tetrafluorophenyl 6-hydrazinopyridine-3-carboxylate (HYNIC-TFP) was synthesized according to the procedure described previously (*24*). To a 2 mL vial were added 30 μL of HYNIC-TFP (3 mg/mL in isopropyl

alcohol), 200 μL of tricine solution (30 mg/mL in 10 mM citrate buffer, pH 5.2), 100 μL of ternary ligand solution (10 mg/mL in 10 mM citrate buffer, pH 5.2), 100 μL of $^{99m}TcO_4^-$ solution (10 mCi/mL in saline), and 25 μL of $SnCl_2 \cdot 2H_2O$ solution (1.0 mg/mL in 0.1 N HCl). The reaction mixture was heated at 95 °C for 15 min followed by cooling on ice for 10 min. Then, the reaction mixture was analyzed by RP-HPLC (solvent system 1).

Radiolabeling of Polypeptides. To a solution of NGA 100 μL (5.0 mg/mL in 0.1 M carbonate buffer, pH 9.0) was added an equal volume of ternary ligand [^{99m}Tc](HYNIC−TFP) complex solution, and the mixture was incubated for 1 h at room temperature. [^{99m}Tc]-(HYNIC−NGA) conjugate was purified by the centrifuged column procedure using Sephadex G-50 equilibrated and eluted with 0.1 M phosphate buffer (pH 7.4). Ternary ligand [^{99m}Tc](HYNIC−Fab) conjugates were prepared according to the procedure described above using 100 μL of Fab solution (5.0 mg/mL in 1 M carbonate buffer, pH 10.0) in place of NGA. Radiochemical yields were assessed by SE-HPLC, CAE, and TLC developed with saline. The levels of HYNIC molecules conjugated per NGA and Fab were determined by measuring the hydrazino groups with *p*-nitrobenzaldehyde according to the method of King et al. (*30*). [^{99m}Tc](HYNIC−Fab)(tricine)$_2$ was prepared by conjugation of 6-hydrazinopyridine-3-carboxylate hydrochloride with Fab fragments, followed by ^{99m}Tc radiolabeling with [^{99m}Tc](tricine)$_2$, according to the procedure described previously (*22*). Direct radioiodination of Fab fragments was performed by the chloramine T method according to the procedure described previously (*4*).

Synthesis of Ternary Ligand [^{99m}Tc](HYNIC−Lysine) Complexes. HYNIC−lysine was synthesized according to the method described previously (*21*). To a 2 mL vial was added 30 μL of HYNIC−lysine (3 mg/mL in 10 mM citrate buffer, pH 5.2), 200 μL of tricine solution (30 mg/mL in 10 mM citrate buffer, pH 5.2), 100 μL of ternary ligand solution (10 mg/mL in 10 mM citrate buffer, pH 5.2), 100 μL of $^{99m}TcO_4^-$ solution (370 MBq/mL in saline), and 25 μL of $SnCl_2 \cdot 2H_2O$ solution (1.0 mg/mL in 0.1 N HCl). The reaction mixture was heated at 95 °C for 15 min. After being cooled at room temperature for 10 min, the reaction mixture was analyzed by RP-HPLC (solvent system 2), CAE, and TLC developed with a mixture of 10% aqueous ammonium chloride−methanol (1:1).

Partition Coefficients of Ternary Ligand [^{99m}Tc]-(HYNIC−Lysine) Complexes. The partition coefficient was measured by mixing each ternary ligand [^{99m}Tc]-(HYNIC−lysine) complex with 3 mL each of 1-octanol and 0.1 M phosphate-buffered saline (pH 4.75). These tubes were left for 20 min at room temperature and then centrifuged for 5 min. Two precisely measured samples (1.0 mL each) from the 1-octanol and buffer layers were counted for radioactivity. The partition coefficient was then determined by calculating the ratio of the radioactivity of the octanol layer to that of the buffer layer.

Plasma Stability of ^{99m}Tc-Labeled Polypeptides. [^{99m}Tc](HYNIC−NGA) conjugates or [^{99m}Tc](HYNIC−Fab) conjugates were diluted 20-fold with freshly prepared murine plasma, and the solution was incubated at 37 °C for 24 h. After 24 h incubation, the radioactivity of each [^{99m}Tc](HYNIC−Fab) conjugate was analyzed by SE-HPLC. After 1, 3, 6, and 24 h incubation, the radioactivity of each [^{99m}Tc](HYNIC−NGA) conjugate was analyzed by CAE.

Immunoreactivity Measurement. The immunoreactivity of [^{99m}Tc](HYNIC−Fab)(tricine)$_2$ and [^{99m}Tc]-(HYNIC−Fab)(tricine)(BP) was determined using ^{125}I-Fab as a control, according to the procedure described previously (*5, 31*). Tumor cells (1.75×10^5 to 2.8×10^6) suspended in 100 μL of Dulbecco's PBS were incubated with 100 μL of [^{99m}Tc](HYNIC−Fab)(tricine)$_2$, [^{99m}Tc]-(HYNIC−Fab)(tricine)(BP), and ^{125}I−Fab for 1 h at 4 °C. After centrifugation at 10000*g* for 5 min, the supernatant was discarded and the radioactivity was determined using a well counter.

In Vivo Studies. Animal studies were conducted in accordance with our institutional guidelines and were approved by Kyoto University Animal Care Committee. Biodistribution studies were performed by the intravenous administration of [^{99m}Tc](HYNIC−NGA) conjugates or [^{99m}Tc](HYNIC−Fab) conjugates to 6-week-old male ddY mice (27−30 g) (*32*). The polypeptide concentrations of [^{99m}Tc](HYNIC−NGA) conjugates and [^{99m}Tc](HYNIC−Fab) conjugates were adjusted to 90 μg/mL and 200 μg/mL, respectively, with saline. Groups of five mice each were administered 9 μg (37−74 KBq) of [^{99m}Tc](HYNIC−NGA) conjugates or 20 μg (37−74 KBq) of [^{99m}Tc](HYNIC−Fab) conjugates prior to sacrificing the animals at 10 or 30 min, 1, 3, 6, or 24 h postinjection by decapitation. Tissues of interest were removed and weighed, and the radioactivity counts were determined with an auto well gamma counter. To determine the amounts and routes of excretion of radioactivity from the body, mice were housed in metabolic cages for 24 h after administration of [^{99m}Tc](HYNIC−NGA) conjugates or [^{99m}Tc](HYNIC−Fab) conjugates, and urine and feces were collected and the radioactivity was determined.

The subcellular distribution of radioactivity in the liver after injection of ^{99m}Tc-labeled NGAs into normal mice was investigated by perfusing the organ in situ with cold 0.25 M sucrose buffered with 10 mM phosphate buffer (pH 7.4) at 1 and 6 h postinjection of [^{99m}Tc](HYNIC−NGA) conjugates (133−266 KBq). The liver was treated according to the procedure described previously (*10, 21*). Briefly, the isolated organ was minced with scissors and suspended in 4 volumes of the same buffer prior to homogenization by hand with a Dounce homogenizer (20 strokes). This was followed by two final strokes in an ice-cooled Potter−Elvehjem homogenizer with a Teflon pestle rotated at 800 rpm. The resulting homogenate was centrifuged twice for 5 min at 340*g* at 4 °C. The isolated supernatant was then layered on top of iso-osmotic (0.25 M sucrose) 37.5% Percoll (9 mL; Pharmacia Biotech) at a density of 1.08 g/mL. After centrifugation at 20000*g* (RP 30 rotor; Hitachi Co. Ltd., Tokyo, Japan) for 90 min at 4 °C, the gradients were collected in 14 fractions. β-Galactosidase was used as a marker enzyme for lysosomes (*33, 34*), and its activity in each fraction was determined using *p*-nitrophenyl β-galactopyranoside as the substrate (*35*). The density and radioactivity counts of the respective fractions were also determined.

The radiolabeled species remaining in the liver at 1 and 6 h postinjection of [^{99m}Tc](HYNIC−NGA) conjugates (133−266 KBq) into normal mice were analyzed according to the procedure described previously (*10, 21*). Briefly, the murine liver was perfused in situ with cold 0.1 M Tris-citrate buffer (pH 6.5) containing 0.15 M NaCl, 0.02% sodium azide, 1 TIU/mL aprotinin, 2 mM benzamidine·HCl, 2 mM iodoacetamide, 1 mM phenylmethylsulfonyl fluoride, and 5 mM diisopropyl fluorophosphate before isolation of the hepatic samples (1 g each). Each tissue sample was placed in a test tube and subjected to three cycles of freezing (dry ice−acetone bath) and thawing. After addition of 5 volumes of the same buffer containing an additional 35 mM β-octyl-glucoside, the

samples were homogenized with a Polytron homogenizer (PT 10−35, Kinematica GmbH, Littau, Switzerland) at full speed with three consecutive 30-s bursts prior to centrifugation at 48000*g* for 20 min at 4 °C (Himac CS-120 Centrifuge; Hitachi Co. Ltd.). The supernatant was separated from the pellet, and the radioactivity was counted. The liver homogenate samples were analyzed immediately by SE-HPLC, CAE, and TLC after filtration through a polycarbonate membrane with a pore diameter of 0.45 μm (Nacalai Tesque). Each sample was also analyzed immediately by RP-HPLC (solvent system 2) after ultrafiltration with a 10 kDa cutoff membrane (Microcon-10; Amicon Grace, Tokyo, Japan).

The radiolabeled species excreted in the urine for 6 h postinjection of [^{99m}Tc](HYNIC−Fab) conjugates were analyzed by SE-HPLC and RP-HPLC (solvent system 2) after filtration through a polycarbonate membrane with a pore diameter of 0.45 μm and a 10 kDa cutoff ultrafiltration membrane, respectively.

Biodistribution Studies in Athymic Mice Bearing Osteogenic Sarcoma. Athymic mice bearing osteogenic sarcoma were also treated intravenously with 100 μL of [^{99m}Tc](HYNIC−Fab)(tricine)$_2$ or [^{99m}Tc](HYNIC−Fab)-(tricine)(BP) (20 μg each), and the animals were sacrificed at 3 or 6 h postinjection (five mice each). Mean weights of mice and tumors used in this study were 18.91 ± 0.95 and 0.23 ± 0.08 g, respectively. Organs of interest were removed and weighed, and the radioactivity in each tissue was determined. Tumor/blood and tumor/kidney ratios were then calculated from the corresponding %ID/g values.

Statistical Analysis. Statistical analysis was performed by applying unpaired *t*-test. $P < 0.05$ was considered statistically significant.

RESULTS

Conjugation of Ternary Ligand Complexes with Polypeptides. Ternary ligand [^{99m}Tc](HYNIC−NGA) conjugates and [^{99m}Tc](HYNIC−Fab) conjugates were prepared by conjugation of ternary ligand [^{99m}Tc](HYNIC-TFP) complexes (active esters) with the ϵ-amine residues of polypeptides. Synthesis of the ternary ligand [^{99m}Tc]-(HYNIC-TFP) complexes was accomplished in one step by direct reduction of [^{99m}Tc]pertechnetate with stannous chloride in the presence of HYNIC-TFP, tricine, and ternary ligands. This gives >75% radiochemical yields of the ^{99m}Tc chelated active esters. RP-HPLC analyses of ternary ligand [^{99m}Tc](HYNIC-TFP) complexes indicated that the major impurity in each reaction was a carboxlic acid of the ^{99m}Tc−HYNIC ternary ligand complex produced due to hydrolysis. The inability to conjugate the carboxylic acid of the ternary ligand ^{99m}Tc−HYNIC complex with polypeptides was confirmed. The conjugation of the ^{99m}Tc−HYNIC active ester with polypeptides was prepared by reaction of the active esters of ^{99m}Tc−HYNIC with ϵ-amine residues of polypeptides at room temperature for 1 h and afforded yields from 30 to 40%. After purification by the centrifuged column procedure, [^{99m}Tc](HYNIC−NGA) conjugates and [^{99m}Tc]-(HYNIC−Fab) conjugates were obtained with radiochemical purities over 95% as determined by SE-HPLC, TLC, and CAE analyses. Average numbers of HYNIC molecules conjugated per NGA and Fab were 1.7 and 0.6, respectively, as determined by measuring the hydrazine groups. In addition, we examined the binding of [^{99m}Tc]-(HYNIC−Fab)(tricine)(BP), [^{99m}Tc](HYNIC−Fab)(tricine)$_2$, and ^{125}I−Fab to KT005 cells, and no differences were observed in the cell-bound radioactivity among the three radiolabeled Fab fragments.

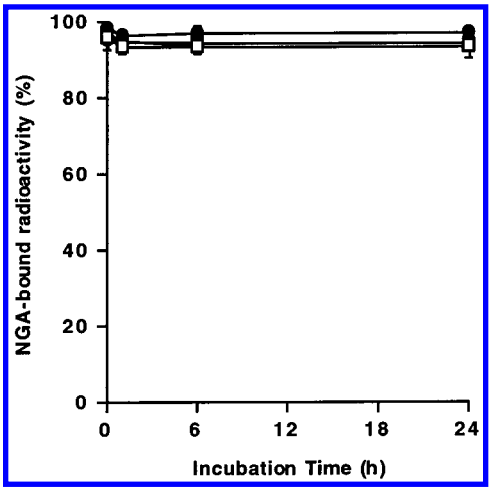

Figure 1. Percent radioactivity in NGA fractions following incubation of [^{99m}Tc](HYNIC−NGA)(tricine)(BP) (●), [^{99m}Tc]-(HYNIC−NGA)(tricine)(AP) (○), [^{99m}Tc](HYNIC−NGA)(tricine)-(NIC) (■), and [^{99m}Tc](HYNIC−NGA)(tricine)(PY) (□) in murine plasma at 37 °C. Values were determined by CAE. Each value represents the mean ± SD of three experiments.

Plasma Stability of [^{99m}Tc](HYNIC−NGA) Conjugates. Percent radioactivity after incubation of [^{99m}Tc]-(HYNIC−NGA) conjugates in freshly prepared murine plasma at 37 °C is shown in Figure 1. The percent radioactivity associated with NGA fractions were unchanged after 24 h incubation in murine plasma.

Biodistribution Study of [^{99m}Tc](HYNIC−NGA) Conjugates in Mice. Radioactivity levels in liver, urine, and feces after intravenous administration of [^{99m}Tc]-(HYNIC−NGA) conjugates are shown in Table 1. At 10 min postinjection, over 90% of the injected radioactivity was accumulated in the liver for all [^{99m}Tc](HYNIC−NGA) conjugates. After this postinjection interval, the radioactivity was gradually eliminated from the liver by hepatobiliary excretion as the major excretion route for the four [^{99m}Tc](HYNIC−NGA) conjugates. ([^{99m}Tc]-(HYNIC−NGA)(tricine)(BP) > [^{99m}Tc](HYNIC−NGA)-(tricine)(AP) > [^{99m}Tc](HYNIC−NGA)(tricine)(NIC) and [^{99m}Tc](HYNIC−NGA)(tricine)(PY)). Low radioactivity levels were observed in tissues other than the liver and intestine throughout the experimental period. No evidence of enterohepatic circulation of the radioactivity was observed.

Analyses of Radioactivity in the Liver. The representative Percoll density gradient centrifugation profiles of radioactivity in the liver at 1 and 6 h postinjection of [^{99m}Tc](HYNIC−NGA)(tricine)(NIC) are shown in Figure 2. Each liver homogenate showed a major radioactivity peak at a density of ca. 1.10 g/mL, which correlated well with the β-galactosidase activity profiles. [^{99m}Tc]-(HYNIC−NGA) conjugates using other ternary ligands (BP, AP, and PY) showed profiles similar to that of [^{99m}Tc](HYNIC−NGA)(tricine)(NIC).

The supernatants of the liver homogenates after injection of all ^{99m}Tc-labeled NGAs were obtained with radiochemical efficiencies of over 90%. Figure 3 shows GPC profiles of the liver supernatants at 1 and 6 h postinjection of [^{99m}Tc](HYNIC−NGA)(tricine)(NIC). These liver supernatants depicted a major radioactivity peak at an elution volume (82.5 mL) close to that of [^{99m}Tc]-(HYNIC−lysine)(tricine)(NIC). The radioactivity peaks in the low molecular weight fractions represented 94.2 and 96.6% of the total radioactivity at 1 and 6 h postinjection, respectively. Under these conditions, the parental [^{99m}Tc](HYNIC−NGA) conjugates had an elution

Table 1. Biodistribution of Radioactivity after Intravenous Administration of ^{99m}Tc-Labeled NGA in Mice[a]

	time after injection					
tissue	10 min	30 min	1 h	3 h	6 h	24 h
			[^{99m}Tc](HYNIC−NGA)(BP)(tricine)			
blood[b]	0.3 ± 0.1	0.4 ± 0.1	0.3 ± 0.0	0.2 ± 0.0	0.1 ± 0.1	0.1 ± 0.0
liver	90.7 ± 1.6	61.0 ± 5.6	43.8 ± 1.9	29.1 ± 3.3	20.3 ± 2.6	12.1 ± 1.1
kidney	0.5 ± 0.2	1.5 ± 0.5	2.0 ± 0.3	0.8 ± 0.2	0.3 ± 0.2	0.2 ± 0.1
intestine	2.6 ± 0.3	19.2 ± 3.9	34.7 ± 1.8	43.9 ± 3.7	33.2 ± 13.3	1.7 ± 0.1
urine						19.0 ± 1.4
feces						53.6 ± 1.8
			[^{99m}Tc](HYNIC−NGA)(AP)(tricine)			
blood[b]	1.0 ± 0.1	0.9 ± 0.1	0.8 ± 0.1	0.4 ± 0.1	0.3 ± 0.0	0.1 ± 0.1
liver	90.5 ± 1.9	72.8 ± 2.5	54.1 ± 2.1	35.8 ± 2.4	25.1 ± 1.8	18.3 ± 1.6
kidney	0.8 ± 0.2	1.6 ± 0.8	1.4 ± 0.8	1.0 ± 0.1	0.5 ± 0.1	0.2 ± 0.0
intestine	1.4 ± 0.2	11.4 ± 1.4	20.8 ± 3.5	33.0 ± 5.5	40.1 ± 6.9	1.5 ± 0.5
urine						26.5 ± 1.9
feces						45.3 ± 1.5
			[^{99m}Tc](HYNIC−NGA)(NIC)(tricine)			
blood[b]	1.1 ± 0.2	0.9 ± 0.2	0.7 ± 0.1	0.5 ± 0.0	0.4 ± 0.1	0.2 ± 0.0
liver	92.6 ± 3.4	71.0 ± 3.4	62.3 ± 1.1	51.1 ± 3.2	47.0 ± 3.5	33.2 ± 1.31
kidney	1.0 ± 0.3	1.0 ± 0.6	1.2 ± 0.5	0.6 ± 0.1	0.5 ± 0.1	0.3 ± 0.0
intestine	1.4 ± 0.2	11.2 ± 1.7	16.4 ± 1.2	23.8 ± 2.6	18.5 ± 3.7	1.8 ± 0.6
urine						22.2 ± 2.3
feces						31.8 ± 1.8
			[^{99m}Tc](HYNIC−NGA)(PY)(tricine)			
blood[b]	1.1 ± 0.1	0.9 ± 0.2	0.7 ± 0.1	0.4 ± 0.0	0.3 ± 0.0	0.2 ± 0.0
liver	91.9 ± 0.5	77.4 ± 1.5	64.3 ± 3.7	52.6 ± 3.8	46.0 ± 3.5	36.0 ± 2.6
kidney	0.7 ± 0.1	0.7 ± 0.3	0.8 ± 0.2	0.8 ± 0.3	0.5 ± 0.1	0.3 ± 0.1
intestine	1.4 ± 0.2	8.0 ± 1.3	15.5 ± 1.4	21.8 ± 2.5	26.7 ± 2.2	1.3 ± 0.2
urine						18.8 ± 1.3
feces						35.2 ± 2.3

[a] Expressed as % injected dose. Each value represents the mean ± SD of five animals. [b] Expressed as % injected dose per gram.

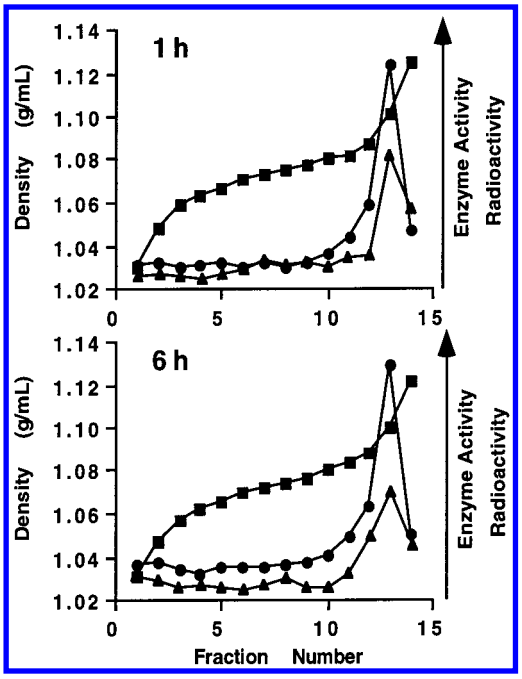

Figure 2. Percoll density gradient centrifugation profiles of liver homogenate at 1 and 6 h postinjection of [^{99m}Tc](HYNIC−NGA)(tricine)(NIC). In both preparations, a single radioactivity peak (●) that coincided with β-galactosidase activity (▲) was detected at a density (■) of ca. 1.10 g/mL.

volume of 32.5 mL. Similar results were obtained when we analyzed the liver supernatants of [^{99m}Tc](HYNIC−NGA) conjugates with the other ternary ligands (BP, AP, and PY). Figure 4 shows RP-HPLC profiles of the liver homogenates at 1 and 6 h postinjection of [^{99m}Tc](HYNIC−NGA)(tricine)(BP), [^{99m}Tc](HYNIC−NGA)(tricine)(AP), [^{99m}Tc](HYNIC−NGA)(tricine)(NIC), and [^{99m}Tc](HYNIC−NGA)(tricine)(PY). All liver supernatants had radiochromatograms identical to the respective ternary ligand [^{99m}Tc](HYNIC−lysine) complexes. These results were also confirmed by co-chromatographic analyses (data not shown). Furthermore, the liver homogenates were analyzed by TLC and CAE, and all liver homogenates showed a single radioactivity peak similar to the respective ternary ligand [^{99m}Tc](HYNIC−lysine) complexes.

Plasma Stability of [^{99m}Tc](HYNIC−Fab) Conjugates. Figure 5 shows SE-HPLC profiles of [^{99m}Tc](HYNIC−Fab) conjugates before and after incubation in freshly prepared murine plasma for 24 h. Although a small peak of radioactivity was observed in large molecular weight fractions (12 and 17 min), each [^{99m}Tc]-(HYNIC−Fab) conjugate showed a major radioactivity peak at the retention time identical to the intact Fab up to 24 h of incubation.

Biodistribution Study of [^{99m}Tc](HYNIC−Fab) Conjugates in Normal Mice. Table 2 shows elimination of radioactivity from the blood and kidneys after administration of [^{99m}Tc](HYNIC−Fab) conjugates. No significant differences were observed in radioactivity levels in the blood among the four Fab conjugates. Radioactivity levels in the kidney reached their peaks at 1 h postinjection for all Fab conjugates, and the radioactivity elimination from the kidney differed with the ternary ligands used. Among the four ternary ligands, [^{99m}Tc](HYNIC−Fab)(tricine)(BP) exhibited the fastest elimination from the kidney. The majority of radioactivity excreted from the body was detected in the urine.

Analyses of Radioactivity in the Urine. Figure 6 shows radiochromatograms of urine samples obtained by 24 h postinjection of [^{99m}Tc](HYNIC−Fab) conjugates. SE-HPLC showed two radioactivity peaks at retention times similar to those of intact [^{99m}Tc](HYNIC−Fab) conjugates (19 min) and low molecular weight compounds (25−28 min). RP-HPLC analyses after filtration with a 10 kDa cutoff membrane showed that the radioactivity in the low

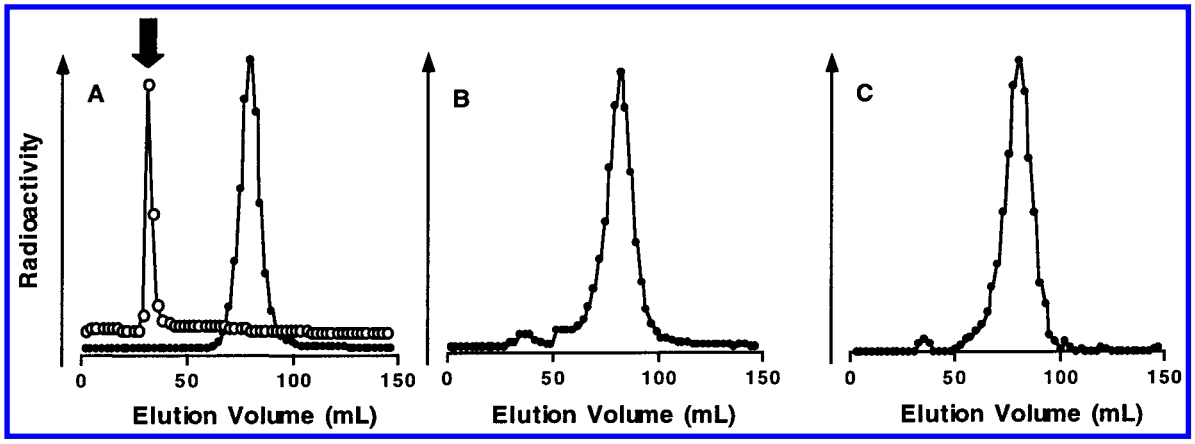

Figure 3. Analyses of liver homogenates at 1 (B) and 6 h (C) postinjection of [^{99m}Tc](HYNIC−NGA)(tricine)(NIC) by GPC. Radiochromatogram of [^{99m}Tc](HYNIC−lysine)(tricine)(NIC) (●) when analyzed by GPC (A). Under these conditions, [^{99m}Tc](HYNIC−NGA)(tricine)(NIC) (○) and blue dextran (↓) eluted at 32.5 mL (A).

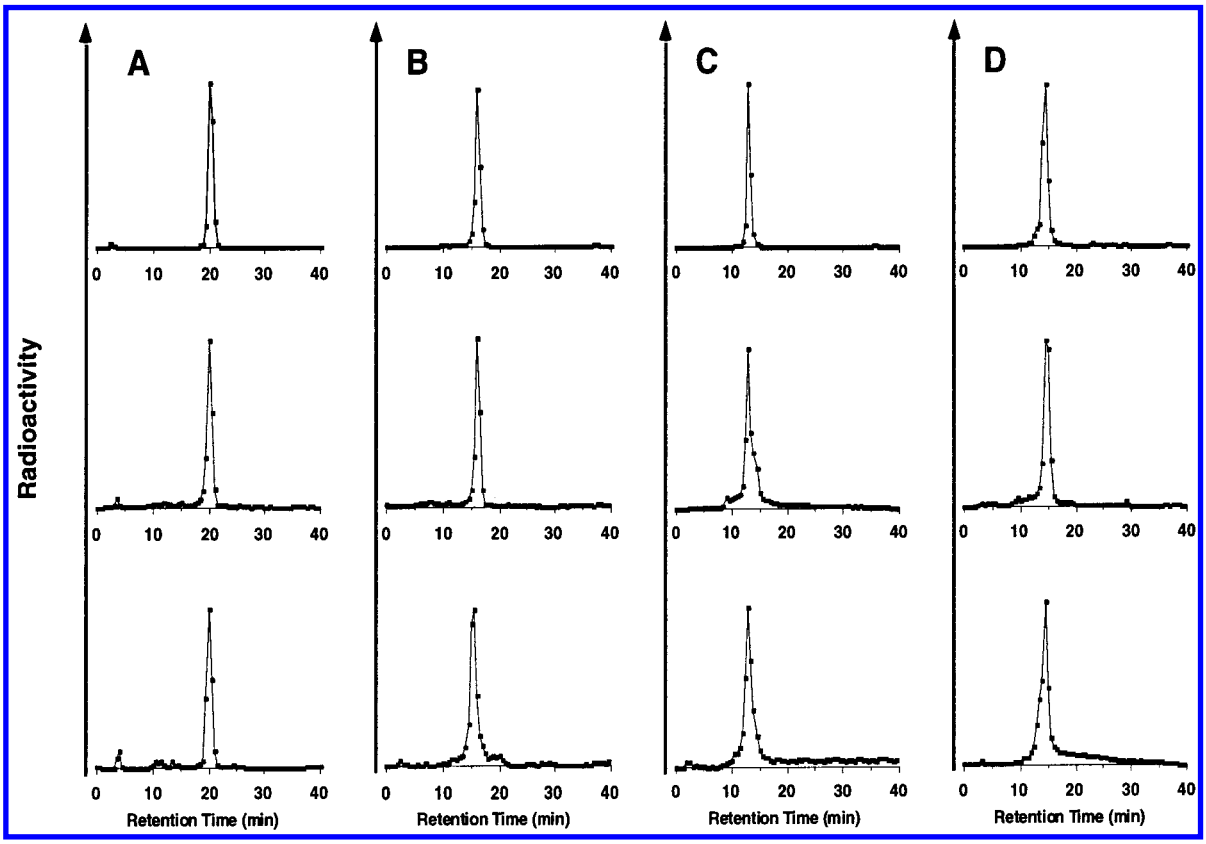

Figure 4. Analyses of liver homogenates at 1 (middle panels) and 6 h (lower panels) postinjection of [^{99m}Tc](HYNIC−NGA)(tricine)-(BP) (A), [^{99m}Tc](HYNIC−NGA)(tricine)(AP) (B), [^{99m}Tc](HYNIC−NGA)(tricine)(NIC) (C) and [^{99m}Tc](HYNIC−NGA)(tricine)(PY) (D) by RP-HPLC using solvent system 2. Radiochromatograms of [^{99m}Tc](HYNIC−lysine)(tricine)(pyridine derivative) when analyzed by RP-HPLC (upper panels).

molecular weight fraction had a retention time identical to that of the respective lysine adduct. These observations were also confirmed by cochromatographic analyses. Furthermore, on TLC, urine samples showed a single radioactivity peak similar to the ternary ligand [^{99m}Tc]-(HYNIC−lysine) complexes.

Partition Coefficients and Retention Times of Ternary Ligand [^{99m}Tc](HYNIC−Lysine) Complexes. The partition coefficients (as log PC values) and the retention times in RP-HPLC of ternary ligand [^{99m}Tc]-(HYNIC−lysine) complexes are summarized in Table 3. The rank order of the lipophilicity of ternary ligand [^{99m}Tc](HYNIC−lysine) complexes was [^{99m}Tc](HYNIC−lysine)(tricine)(BP) > [^{99m}Tc](HYNIC−lysine)(tricine)(AP) > [^{99m}Tc](HYNIC−lysine)(tricine)(PY) > [^{99m}Tc](HYNIC−lysine)(tricine)(NIC).

Biodistribution Study in Athymic Mice Bearing Osteogenic Sarcoma. Figure 7 shows the radioactivity levels in blood, kidney, and tumor at 3 and 6 h after administration of [^{99m}Tc](HYNIC−Fab)(tricine)(BP) and [^{99m}Tc](HYNIC−Fab)(tricine)$_2$ in athymic mice bearing osteogenic sarcoma. [^{99m}Tc](HYNIC−Fab)(tricine)(BP) showed significant reduction of radioactivity levels in the blood and kidney at both postinjection times compared with [^{99m}Tc](HYNIC−Fab)(tricine)$_2$, although [^{99m}Tc]-(HYNIC−Fab)(tricine)(BP) showed lower radioactivity

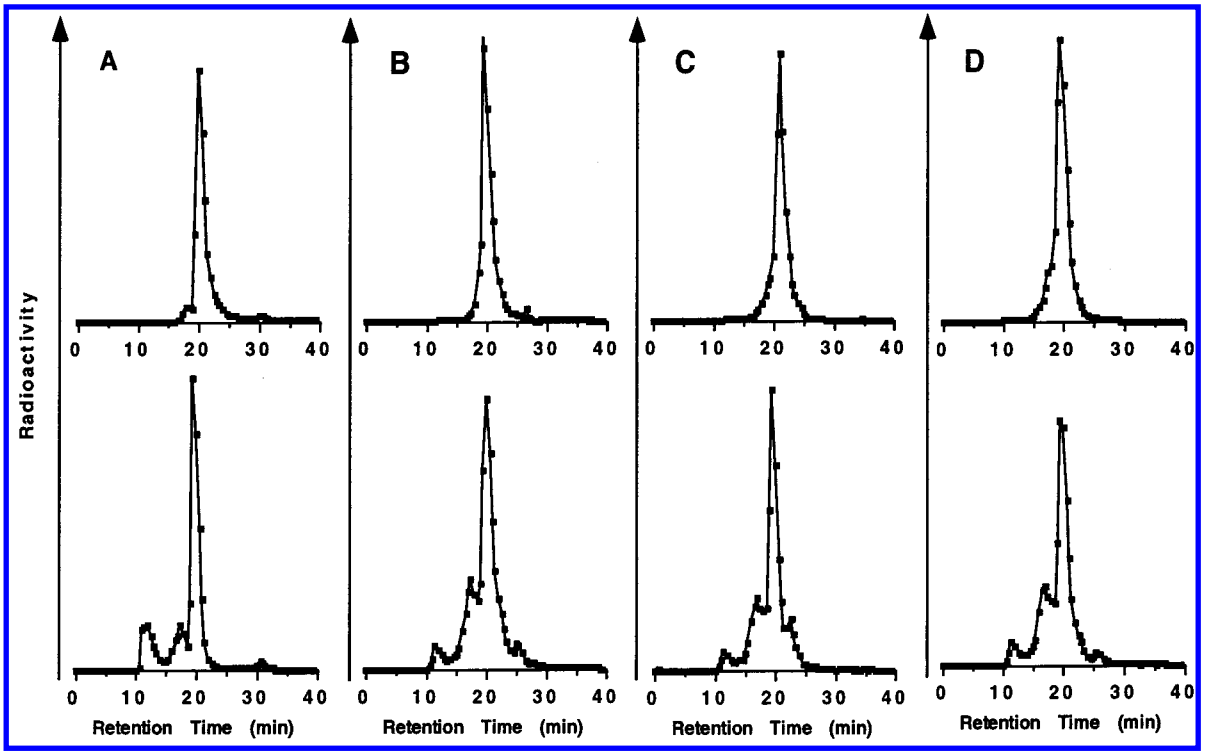

Figure 5. SE-HPLC profiles of radioactivity in murine plasma before (upper panels) and after 24 h incubation (lower panels) at 37 °C of [^{99m}Tc](HYNIC−Fab)(tricine)(BP) (A), [^{99m}Tc](HYNIC−Fab)(tricine)(AP) (B), [^{99m}Tc](HYNIC−Fab)(tricine)(NIC) (C) and [^{99m}Tc](HYNIC−Fab)(tricine)(PY) (D). Under these conditions, thyroglobulin (670 kDa), glutamate dehydrogenase (290 kDa), IgG (150 kDa), bovine serum albumin (68 kDa), Fab fragment (5 kDa) and cytochrome C (13 kDa) had retention times of 12, 14.5, 16, 18, 19, and 21 min, respectively, on SE-HPLC.

Table 2. Biodistributions of Radioactivity after Intravenous Administration of ^{99m}Tc-Labeled Fab in Mice[a]

	time after injection					
tissue	10 min	30 min	1 h	3 h	6 h	24 h
			[^{99m}Tc](HYNIC−Fab)(tricine)(BP)			
blood	21.1 ± 1.2	12.2 ± 2.1	7.8 ± 1.1	3.5 ± 0.6	1.9 ± 0.3	0.4 ± 0.1
liver	7.0 ± 0.4	6.9 ± 1.5	6.7 ± 1.3	6.6 ± 1.4	5.2 ± 1.0	2.8 ± 0.4
kidney	31.5 ± 3.8	52.2 ± 5.4	54.7 ± 5.3	37.1 ± 2.3	22.5 ± 1.9	6.9 ± 1.1
intestine	1.1 ± 0.1	1.3 ± 0.2	1.7 ± 0.4	2.1 ± 0.3	2.9 ± 0.6	0.4 ± 0.1
urine[b]						51.7 ± 3.1
feces[b]						11.6 ± 1.0
			[^{99m}Tc](HYNIC−Fab)(tricine)(AP)			
blood	22.5 ± 0.6	14.1 ± 0.7	8.2 ± 1.1	3.1 ± 0.5	2.1 ± 0.1	0.5 ± 0.2
liver	6.2 ± 0.1	6.2 ± 0.7	5.7 ± 0.8	4.4 ± 0.9	5.0 ± 0.3	3.4 ± 0.5
kidney	36.3 ± 4.4	51.2 ± 3.1	65.9 ± 6.7	47.2 ± 7.9	29.0 ± 2.9	13.1 ± 2.5
intestine	1.0 ± 0.2	1.3 ± 0.2	1.1 ± 0.1	1.2 ± 0.3	1.4 ± 0.3	1.6 ± 1.2
urine[b]						58.1 ± 3.0
feces[b]						8.2 ± 3.0
			[^{99m}Tc](HYNIC−Fab)(tricine)(NIC)			
blood	24.3 ± 1.1	13.4 ± 0.8	7.7 ± 0.7	4.2 ± 0.4	1.8 ± 0.2	0.4 ± 0.2
liver	6.7 ± 0.6	5.7 ± 0.5	6.4 ± 1.3	6.3 ± 0.8	5.3 ± 1.6	4.7 ± 1.1
kidney	30.3 ± 1.0	48.9 ± 2.4	58.5 ± 3.9	50.1 ± 5.9	27.0 ± 2.7	15.2 ± 2.0
intestine	1.1 ± 0.1	1.1 ± 0.1	1.2 ± 0.2	1.4 ± 0.3	1.3 ± 0.2	0.6 ± 0.1
urine[b]						60.7 ± 0.4
feces[b]						5.4 ± 1.2
			[^{99m}Tc](HYNIC−Fab)(tricine)(PY)			
blood	23.7 ± 1.4	14.5 ± 2.4	8.8 ± 1.7	3.9 ± 0.2	2.4 ± 0.3	0.6 ± 0.2
liver	4.3 ± 0.4	4.9 ± 0.6	5.5 ± 0.9	4.6 ± 0.5	4.0 ± 0.5	2.6 ± 0.4
kidney	27.7 ± 2.5	54.8 ± 9.8	73.1 ± 5.8	58.7 ± 3.3	44.0 ± 5.0	15.1 ± 1.9
intestine	0.9 ± 0.1	1.3 ± 0.1	1.4 ± 0.2	1.0 ± 0.1	0.9 ± 0.2	0.7 ± 0.1
urine[b]						57.4 ± 4.2
feces[b]						3.8 ± 1.0

[a] Expressed as % injected dose per gram. Each value represents the mean ± SD of five animals. [b] Expressed as % injected dose.

levels in the tumor than [^{99m}Tc](HYNIC−Fab)(tricine)$_2$. Thus, [^{99m}Tc](HYNIC−Fab)(tricine)(BP) provided significantly higher tumor/blood and tumor/kidney ratios of radioactivity than [^{99m}Tc](HYNIC−Fab)(tricine)$_2$ (Figure 8).

DISCUSSION

Although the relationship between solute lipophilicity and permeation across the cell membrane is well-known, there have been no systematic studies of the effects of

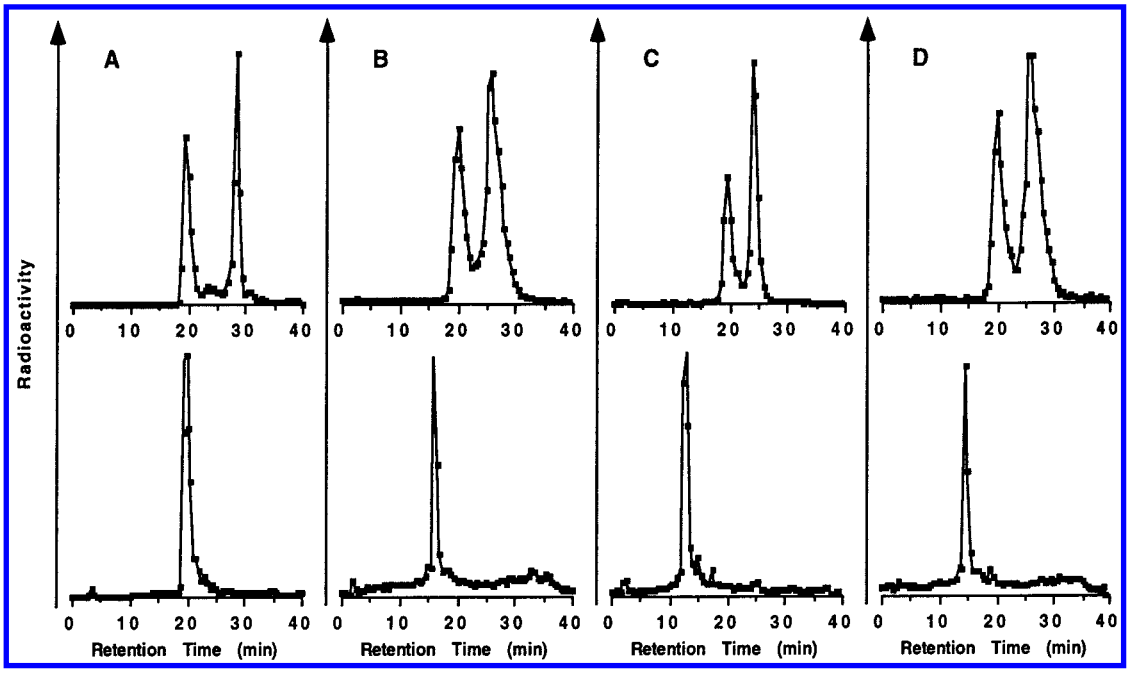

Figure 6. Radiochromatograms of urine samples obtained for 6 h postinjection of [^{99m}Tc](HYNIC−Fab)(tricine)(BP) (A), [^{99m}Tc]-(HYNIC−Fab)(tricine)(AP) (B), [^{99m}Tc](HYNIC−Fab)(tricine)(NIC) (C), and [^{99m}Tc](HYNIC−Fab)(tricine)(PY) (D) by SE-HPLC (upper panels) and RP-HPLC using solvent system 2 (lower panels). Urine samples were analyzed by SE-HPLC after filtration through a polycarbonate membrane with a pore diameter of 0.45 μm and by RP-HPLC after ultrafiltration through a 10 kDa cutoff membrane.

Table 3. Partition Coefficients and RP-HPLC Data of [^{99m}Tc](HYNIC−Lysine) Ternary Ligand Complexes.

radiometabolite	log PC[a]	retention time (min)[b]
[^{99m}Tc](HYNIC−lysine)(BP)(tricine)	−2.21 ± 0.03	20.3
[^{99m}Tc](HYNIC−lysine)(AP)(tricine)	−2.37 ± 0.05	16.1
[^{99m}Tc](HYNIC−lysine)(PY)(tricine)	−2.73 ± 0.06	14.3
[^{99m}Tc](HYNIC−lysine)(NIC)(tricine)	−2.93 ± 0.16	13.2

[a] Octanol/buffer (0.1 M phosphate buffered saline, pH 4.75) partition coefficients. Each value represents the mean ± SD of three experiments. [b] Using solvent system 2.

the lipophilicity of radiometabolites on their elimination rates from the tissue after administration of radiolabeled polypeptides. A previous study in our laboratory indicated that radiometabolites with different lipophilicity should show different permeation rates through the hepatic lysosomal membrane (*11*). As the pyridine derivative coligands could alter the lipophilicity of ^{99m}Tc−HYNIC-labeled metabolites, we used four pyridine derivatives as ternary ligands to prepare ^{99m}Tc−HYNIC-labeled polypeptides for further investigation of the effects of the lipophilicity of radiometabolites on the radioactivity elimination from the tissue.

The procedure for synthesis of ternary ligand complexes and subsequent conjugation with polypeptides has been well established as described previously (*24*). The selective conjugation of ternary ligand [^{99m}Tc](HYNIC-TFP) complexes to the ϵ-amine residues of polypeptides was supported by generating lysine adducts of HYNIC as radiometabolites (Figures 4 and 6). The rapid and quantitative accumulation of all ^{99m}Tc-labeled NGAs (Table 1) and the lack of changes in immunoreactivity of ^{99m}Tc-labeled Fab suggested that the biological reactivity of parental proteins was retained after conjugation of preformed ^{99m}Tc−HYNIC complexes.

The stability of the ^{99m}Tc−HYNIC-labeled polypeptides designed in the present study was evaluated by incubation in murine plasma. After incubation of all [^{99m}Tc]-(HYNIC−NGA) conjugates in murine plasma, almost all radioactivity was observed in the NGA fractions (Figure 1). Plasma incubation of four [^{99m}Tc](HYNIC−Fab) conjugates showed high stability of the ternary ligand ^{99m}Tc complexes against exchange reaction with plasma proteins (Figure 5), whereas [^{99m}Tc](HYNIC−Fab)(tricine)$_2$ showed significantly larger amounts of higher molecular weight radiolabeled species (over 600 kDa) (*22*). The high degree of stability of ^{99m}Tc−HYNIC ternary ligand complex against exchange reaction with plasma proteins was reflected by the faster blood clearance of ternary ligand [^{99m}Tc](HYNIC−Fab) conjugates as compared with [^{99m}Tc](HYNIC−Fab)(tricine)$_2$ (*21*). The lack of significant differences in the blood clearance of radioactivity among the four ^{99m}Tc-labeled Fab fragments indicated that the association of ternary ligand complexes with polypeptides did not affect the pharmacokinetics of the parental Fab.

Stability of radiometabolites was investigated by analysis of radiometabolites generated in hepatocytes after administration of [^{99m}Tc](HYNIC−NGA) conjugates. On GPC and RP-HPLC analyses, all liver homogenates at 1 h postinjection of four [^{99m}Tc](HYNIC−NGA) conjugates showed a single radioactivity peak at a position identical to that of the respective ternary ligand [^{99m}Tc](HYNIC−lysine) complex (Figures 3 and 4). The radiochromatograms were unchanged for up to 6 h postinjection. These findings indicated that the ternary ligand complexes remained stable against exchange reaction with proteins in the lysosomes even after catabolism to lysine adducts. Therefore, elimination rates from the liver after injection of ternary ligand [^{99m}Tc](HYNIC−NGA) conjugates would reflect those of the respective radiometabolites.

Radioactivity elimination from the tissues after administration of ^{99m}Tc−HYNIC-labeled NGAs varied with the ternary ligands used. As shown in Table 1, [^{99m}Tc]-(HYNIC−NGA) conjugates prepared using four ternary ligands were eliminated from the liver in the order of increasing lipophilicity of radiometabolites, ternary ligand [^{99m}Tc](HYNIC−lysine) complexes (Table 3). As almost all radioactivity of the [^{99m}Tc](HYNIC−lysine) complexes existed in the lysosomes of hepatocytes (Figure 2), the

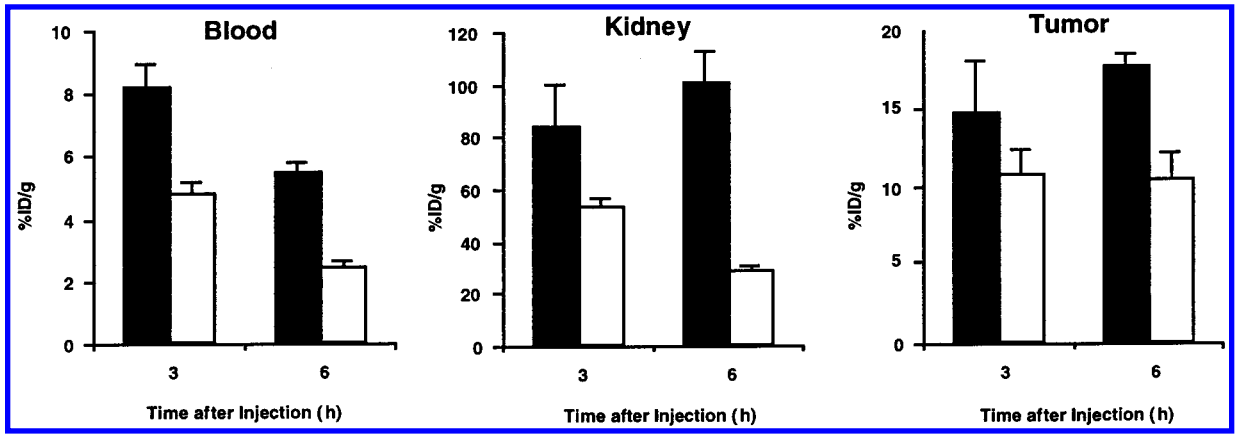

Figure 7. Comparative biodistribution of radioactivity at 3 and 6 h postinjection of [^{99m}Tc](HYNIC−Fab)(tricine)(BP) (open columns) and [^{99m}Tc](HYNIC−Fab)(tricine)$_2$ (closed columns) in athymic mice bearing osteogenic sarcoma. Each value represents the mean ± SD of five animals.

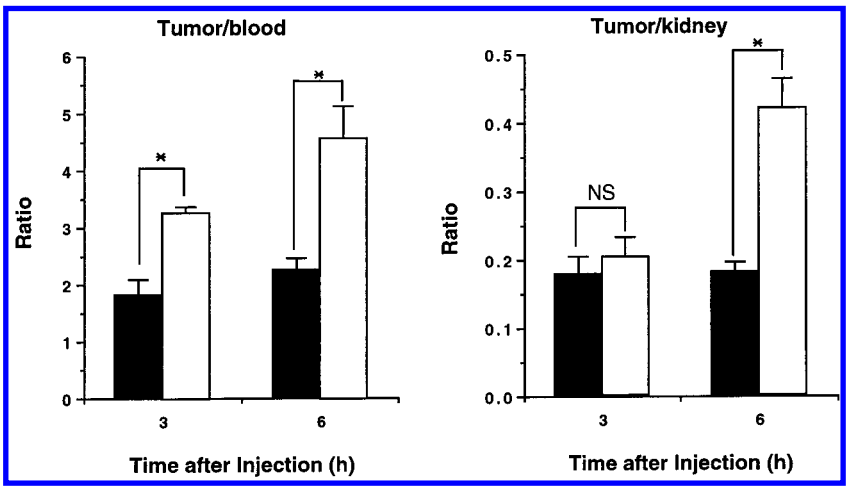

Figure 8. Tumor/blood and tumor/kidney ratios of the radioactivity at 3 and 6 h postinjection of [^{99m}Tc](HYNIC−Fab)(tricine)(BP) (open columns) and [^{99m}Tc](HYNIC−Fab)(tricine)$_2$ (closed columns) in athymic mice bearing osteogenic sarcoma. Significance was determined by unpaired *t*-test (*: $p < 0.01$, NS: not significant). Each value represents the mean ± SD of five animals.

lipophilicy of radiometabolites would affect the permeation rates through the lysosomal membrane.

Radioactivity elimination from the kidney after injection of ternary ligand [^{99m}Tc](HYNIC−Fab) conjugates differed with the ternary ligands used (Table 2). Radioactivity excreted in the urine existed as intact radiolabeled Fab fragments and ternary ligand [^{99m}Tc](HYNIC−lysine) complexes (Figure 6). As elimination of four [^{99m}Tc](HYNIC−Fab) conjugates from the kidney would be similar, the differences in radioactivity elimination from the kidney after injection of the four [^{99m}Tc](HYNIC−Fab) conjugates could reflect differences in elimination rates of the radiometabolites. Indeed, radioactivity elimination from the kidney after injection of ternary ligand [^{99m}Tc](HYNIC−Fab) conjugates increased in the order of increasing lipophilicity of the radiometabolites, ternary ligand [^{99m}Tc](HYNIC−lysine) complexes (Tables 2 and 3).

These findings indicated that the lipophilicity of radiometabolites plays an important role in the radioactivity elimination rates from the tissues after administration of radiolabeled polypeptides. The present findings also suggested that radiolabeling reagents producing lipophilic radiometabolites by lysosomal proteolysis would be useful for the enhancement of the target/nontarget ratio of radioactivity levels when using radiolabeled polypeptides that are not internalized within the target cells. To confirm the usefulness of this approach, the biodistribution study in athymic mice was performed using Fab fragments that are not internalized within tumor cells (Figures 7 and 8). BP was selected as a ternary ligand, as [^{99m}Tc](HYNIC−lysine)(tricine)(BP) exhibited the most rapid elimination from the tissues. Although [^{99m}Tc](HYNIC−Fab)(tricine)(BP) showed lower radioactivity levels in the tumor compared with [^{99m}Tc](HYNIC−Fab)(tricine)$_2$, [^{99m}Tc](HYNIC−Fab)(tricine)(BP) showed significant increases of the tumor/blood and tumor/kidney ratios due to significant reduction of the radioactivity levels in the blood and kidney (Figure 8).

Determination of the relationships between the lipophilicity of radiometabolites and their elimination rates from the tissues would facilitate design of radiolabeling reagents with a metabolizable linkage. However, it is necessary for enhancement of the target/nontarget ratio not only to release the lipophilic radiometabolites in the nontarget tissues but also to stabilize the metabolizable linkage in plasma. As chemical structures of linkages and radiolabels attached to the metabolizable bonds significantly affect the stability of these bonds in radiolabeled polypeptides (*36*), radiolabeling reagents producing lipophilic radiometabolites by lysosomal proteolysis might be more useful than those that require cleavage of a metabolizable linkage.

The present findings also suggested that the reagents to radiolabel polypeptides producing hydrophilic radiometabolites would be required when applied to internalizable (poly)peptides within target cells. Use of chemically modified (poly)peptides in combination with these re-

agents could achieve further enhancement of the target/nontarget ratio.

In conclusion, the present study indicated that the lipophilicity of the radiometabolites derived from radiolabeled polypeptides constitutes one important factor affecting the elimination rate from the tissues. As pyridine derivatives could serve as stable ternary ligands in ^{99m}Tc−HYNIC-labeled polypeptides and alter the physicochemical properties of radiometabolites, the use of pyridine derivatives as ternary ligands for preparation of ^{99m}Tc−HYNIC-labeled polypeptides might be applicable for controlling the radioactivity pharmacokinetics. The findings of the present study will be useful to enhance the target/nontarget ratios of polypeptide radiopharmaceuticals.

LITERATURE CITED

(1) Haseman, M. K., Goodwin, D. A., Meares, C. F., Kaminski, M. S., Wensel, T. G., McCall, M. J., and Levy, R. (1986) Metabolizable ^{111}In chelate conjugated anti-idiotype monoclonal antibody for radioimmunodetection of lymphoma in mice. *Eur. J. Nucl. Med. 12*, 455−460.

(2) Paik, C. H., Quadri, S. M., and Reba, R. C. (1989) Interposition of different chemical linkages between antibody and ^{111}In-DTPA to accelerate clearance from nontarget organs and blood. *Nucl. Med. Biol. 16*, 475−481.

(3) Weber, R. W., Boutin, R. H., Nedelman, M. A., Lister-James, J., and Dean, R. T. (1990) Enhanced kidney clearance with an ester-linked ^{99m}Tc-radiolabeled antibody Fab′-chelator conjugate. *Bioconjugate Chem. 1*, 431−437.

(4) Arano, Y., Wakisaka, K., Ohmomo, Y., Uezono, T., Akizawa, H., Nakayama, M., Sakahara, H., Tanaka, C., Konishi, J., and Yokoyama, A. (1996) Assessment of radiochemical design of antibodies using an ester bond as the metabolizable linkage: evaluation of maleimidoethyl 3-(tri-*n*-butylstannyl)-hippurate as a radioiodination reagent of antibodies for diagnostic and therapeutic applications. *Bioconjugate Chem. 7*, 628−637.

(5) Arano, Y., Inoue, T., Mukai, T., Wakisaka, K., Sakahara, H., Konishi, J., and Yokoyama, A. (1994) Discriminated release of a hippurate-like radiometal chelate in nontarget tissues for target-selective radioactivity localization using pH-dependent dissociation of reduced antibody. *J. Nucl. Med. 35*, 326−333.

(6) Khaw, B. A., Klibanov, A., O'Donnell, S. M., Saito, T., Nossiff, N., Slinkin, M. A., Newell, J. B., Strauss, H. W., and Torchilin, V. P. (1991) Gamma imaging with negatively charge-modified monoclonal antibody: modification with synthetic polymers. *J. Nucl. Med. 32*, 1742−1751.

(7) Gangopadhyay, A., Petrick, A. T., and Thomas, P. (1996) Modification of antibody isoelectric point affects biodistribution of 111-indium-labeled antibody. *Nucl. Med. Biol. 23*, 257−261.

(8) Kim, I. S., Yoo, T. M., Kobayashi, H., Kim, M. K., Le, N., Wang, Q. C., Pastan, I., Carrasquillo, J. A., and Paik, C. H. (1999) Chemical modification to reduce renal uptake of disulfide-bonded variable region fragment of anti-Tac monoclonal antibody labeled with ^{99m}Tc. *Bioconjugate Chem. 10*, 447−453.

(9) Akizawa, H., Arano, Y., Mifune, M., Iwado, A., Saito, Y., Mukai, T., Uehara, T., Ono, M., Fujioka, Y., Ogawa, K., Kiso, Y., and Saji, H. (in press) Effect of molecular charges on renal uptake of ^{111}In-DTPA conjugated peptides. *Nucl. Med. Biol.*

(10) Arano, Y., Mukai, T., Uezono, T., Wakisaka, K., Motonari, H., Akizawa, H., Taoka, Y., and Yokoyama, A. (1994) A biological method to evaluate bifunctional chelating agents to label antibodies with metallic radionuclides. *J. Nucl. Med. 35*, 890−898.

(11) Arano, Y., Mukai, T., Akizawa, H., Uezono, T., Motonari, H., Wakisaka, K., Kairiyama, C., and Yokoyama, A. (1995) Radiolabeled metabolites of protein play a critical role in radioactivity elimination from the liver. *Nucl. Med. Biol. 22*, 555−564.

(12) Akizawa, H., Arano, Y., Uezono, T., Ono, M., Fujioka, Y., Uehara, T., Yokoyama, A., Akaji, K., Kiso, Y., and Saji, H. (1998) Renal metabolism of ^{111}In-DTPA-D-Phe^1-octreotide in vivo. *Bioconjugate Chem. 9*, 662−670.

(13) Mukai, T., Arano, Y., Nishida, K., Sasaki, H., Saji, H., and Nakamura, J. (1999) In-vivo evaluation of indium-111-diethylenetriaminepentaacetic acid labeling for determining the sites and rates of protein catabolism in mice. *J. Pharm. Pharmacol. 51*, 15−20.

(14) Abrams, M. J., Juweid, M., tenKate, C. I., Schwartz, D. A., Hauser, M. M., Gaul, F. E., Fuccello, A. J., Rubin, R. H., Strauss, H. W., and Fischman, A. J. (1990) Technetium-99m-human polyclonal IgG radiolabeled via the hydrazino nicotinamide derivative for imaging focal sites of infection in rats. *J. Nucl. Med. 31*, 2022−2028.

(15) Claessens, R. A., Koenders, E. B., Oyen, W. J. G., and Corstens, F. H. (1996) Retention of technetium-99m in infectious foci in rats after release from technetium-99m labeled human nonspecific polyclonal immunoglobulin G: a dual-label study with hydrazinonicotinamido and iminothiolano immunoglobulin. *Eur. J. Nucl. Med. 23*, 1536−1539.

(16) Ultee, M. E., Bridger, G. J., Abrams, M. J., Longley, C. B., Burton, C. A., Larsen, S. K., Henson, G. W., Padmanabhan, S., Gaul, F. E., and Schwartz, D. A. (1997) Tumor imaging with technetium-99m-labeled hydrazinonicotinamide-Fab′ conjugates. *J. Nucl. Med. 38*, 133−138.

(17) Verbeke, K., Hjelstuen, O., Debrock, E., Cleynhens, B., De Roo, M., and Verbruggen, A. (1995) Comparative evaluation of ^{99}Tc^m-Hynic-HSA and ^{99}Tc^m-MAG$_3$−HSA as possible blood pool agents. *Nucl. Med. Commun. 16*, 942−957.

(18) Fischman, A. J., Rauh, D., Solomon, H., Babich, J. W., Tompkins, R. G., Kroon, D., Strauss, H. W., and Rubin, R. H. (1993) In vivo bioactivity and biodistribution of chemotactic peptide analogues in nonhuman primates. *J. Nucl. Med. 34*, 2130−2134.

(19) Liu, S., Edwards, D. S., Looby, R. J., Harris, A. R., Poirier, M. J., Barrett, J. A., Heminway, S. J., and Carroll, T. R. (1996) Labeling a hydrazino nicotinamide-modified cyclic IIb/IIIa receptor antagonist with ^{99m}Tc using aminocarboxylates as coligands. *Bioconjugate Chem. 7*, 63−71.

(20) Decristoforo, C. and Mather, S. J. (1999) 99m-Technetium-labeled peptide-HYNIC conjugates: effects of lipophilicity and stability on biodistribution. *Nucl. Med. Biol. 26*, 389−396.

(21) Ono, M., Arano, Y., Uehara, T., Fujioka, Y., Ogawa, K., Namba, S., Mukai, T., Nakayama, M., and Saji, H. (1999) Intracellular metabolic fate of radioactivity after injection of technetium-99m-labeled hydrazino nicotinamide derivatized proteins. *Bioconjugate Chem. 10*, 386−394.

(22) Ono, M., Arano, Y., Mukai, T., Uehara, T., Fujioka, Y., Ogawa, K., Namba, S., Nakayama, M., Saga, T., Konishi, J., Horiuchi, K., Yokoyama, A., and Saji, H. (2001) Plasma protein binding of ^{99m}Tc-labeled hydrazino nicotinamide derivatized polypeptides and peptides. *Nucl. Med. Biol. 28*, 155−164.

(23) Liu, S., Edwards, D. S., and Harris, A. R. (1998) A novel ternary ligand system for ^{99m}Tc-labeling of hydrazino nicotinamide-modified biologically active molecules using imine-N-containing heterocycles as coligands. *Bioconjugate Chem. 9*, 583−595.

(24) Ono, M., Arano, Y., Mukai, T., Fujioka, Y., Ogawa, K., Uehara, T., Saga, T., Konishi, J., and Saji, H. (2001) ^{99m}Tc−HYNIC-derivatized ternary ligand complexes for ^{99m}Tc-labeled polypeptides of low in vivo protein binding. *Nucl. Med. Biol. 28*, 215−224.

(25) Lee, Y. C., Stowell, C. P., and Krantz, M. J. (1976) 2-imino-2-methoxyethyl 1-thioglycosides: new reagents for attaching sugars to proteins. *Biochemistry 15*, 3956−3963.

(26) Stowell, C. P. and Lee, Y. C. (1980) Preparation of some new neoglycoproteins by amidination of bovine serum albumin using 2-imino-2-methoxyethyl 1-thioglycosides. *Biochemistry 19*, 4899−4904.

(27) Dubois, M., Gilles, K. A., Hamilton, J. K., Rebers, P. A., and Smith, F. (1956) Colorimetric method for determination of sugars and related substances. *Anal. Chem. 28*, 350−356.

(28) Gorevic, P. D., Prelli, F. C., and Frangione, B. (1985) Purification and characterization of serum immunoglobulins. *Methods Enzymol. 116*, 3−25.
(29) Hosoi, S., Nakamura, T., Higashi, S., Yamamuro, T., Toyama, S., Shinomiya, K., and Mikawa, H. (1982) Detection of human osteosarcoma-associated antigen(s) by monoclonal antibodies. *Cancer Res. 42*, 654−659.
(30) King, T. P., Zhao, S. W., and Lam, T. (1986) Preparation of protein conjugates via intermolecular hydrazone linkage. *Biochemistry 25*, 5774−5779.
(31) Koizumi, M., Endo, K., Kunimatsu, M., Sakahara, H., Nakashima, T., Kawamura, Y., Watanabe, Y., Saga, T., Konishi, J., Yamamuro, T., Hosoi, S., Toyama, S., Arano, Y., and Yokoyama A. (1988) ^{67}Ga-labeled antibodies for immunoscintigraphy and evaluation of tumor targeting of drug-antibody conjugate in mice. *Cancer Res. 48*, 1189−1194.
(32) Imai, S., Morimoto, J., Tsubura, T., Esaki, K., Michalides, R., Holms, R. S., Deimling, O., and Higlgers, J. (1986) Genetic marker patterns and endogenous mammary tumor virus genes in inbred mouse strains in Japan. *Exp. Anim. 35*, 263−276.
(33) Alquier, C., Guenin, P., Munari-Silem, Y., Audebet, C., and Rousset, B. (1985) Isolation of pig thyroid lysosomes. *Biochem. J. 232*, 529−537.
(34) Caimi, L., Marchesini, S., Aleo, M. F., Bresciani, R., Monti, E., Casella, A., Guidici, M. L., and Preti, A. (1989) Rapid preparation of a distinct lysosomal population from myelinating mouse brain using Percoll gradients. *J. Neurochem. 52*, 1722−1728.
(35) Distler, J. and Jourdian, G. W. β-Galactosidase from bovine testes. *Methods Enzymol. 50*, 514−520.
(36) Arano Y, Wakisaka K, Mukai T, Uezono T, Motonari H, Akizawa H, Kairiyama C, Ohmomo Y, Tanaka C, Ishiyama M, Sakahara H, Konishi J, and Yokoyama A. (1996) Stability of a metabolizable ester bond in radioimmunoconjugates. *Nucl. Med. Biol. 23*, 129−136.

BC010043K